DALTON
FULL PAPER

Acetylide generation and coupling on electron-rich Ru_3 clusters

Paul J. Low,*[a,b] Tim M. Hayes,[a] Konstantin A. Udachin,[b] Andres E. Goeta,[a] Judith A. K. Howard,[a] Gary D. Enright[b] and Arthur J. Carty*[b,c]

[a] *Department of Chemistry, University of Durham, South Road, Durham, UK DH1 3LE. E-mail: p.j.low@durham.ac.uk*
[b] *Steacie Institute for Molecular Sciences, National Research Council of Canada, 100 Sussex Drive, Ottawa, Ontario, K1A 0R6, Canada*
[c] *Ottawa-Carleton Research Institute, Department of Chemistry, University of Ottawa, Ottawa, Ontario, K1N 6N5, Canada*

Received 21st September 2001, Accepted 6th February 2002
First published as an Advance Article on the web 6th March 2002

Thermolysis of $[Ru_3(CO)_{10}(Ph_2PC{\equiv}CBu^t)_2]$ (**1a**) gives the 48-e cluster $[Ru_3(\mu\text{-}\eta^1,\eta^2\text{-}C{\equiv}CBu^t)_2(\mu\text{-}PPh_2)_2(CO)_6]$ (**4**), which readily adds CO or PPh_3 to give the corresponding 50-e clusters $[Ru_3(\mu\text{-}\eta^1,\eta^2\text{-}C{\equiv}CBu^t)_2(\mu\text{-}PPh_2)_2(CO)_6(L)]$ (L = CO, **5a**, PPh_3, **6**) while thermolysis of $[Ru_3(CO)_{10}(Ph_2PC{\equiv}CPh)(Ph_2PC{\equiv}CR)]$ (R = Ph, **1b**; Bu^t **1c**) affords 50-e $[Ru_3(\mu\text{-}PPh_2)(\mu\text{-}\eta^1,\eta^2\text{-}C{\equiv}CPh)(\mu\text{-}\eta^1,\eta^2\text{-}C{\equiv}CR)(CO)_7]$ (**5b**, **5c**) directly, which convert smoothly to the 48-e diyne clusters $[Ru_3(\mu\text{-}\eta^2\text{-}PhC_2C{\equiv}CR)(\mu\text{-}PPh_2)_2(CO)_7]$ (**7b**, **7c**). In the case of $[Ru_3(CO)_{10}(Ph_2PC{\equiv}CPh)_2]$ the compound $\{Ru_2[\eta^1,\eta^1 : \eta^2,\eta^2\text{-}PhCC(PPh_2)CCPh](CO)_5\}(\mu\text{-}PPh_2)[Ru(CO)_3]$ (**8**) is also obtained.

Introduction

Examples of intra-molecular coupling reactions of acetylide ligands leading to the formation of diyne and polyyne ligands are relatively rare in late-transition metal cluster chemistry.[1–4] More often, late-transition metal clusters bearing conjugated polyyne ligands are prepared by reactions of a polyyne $R(C{\equiv}C)_nR'$ with a metal reagent.[5] We were interested in exploring acetylide coupling reactions as part of a broader study of transition metal clusters bearing polyyne ligands,[6] and therefore required access to a range of metal clusters featuring multiple acetylide ligands.

The P–C bonds in coordinated phosphinoacetylenes, $R_2PC{\equiv}CR'$, are sensitive to cleavage and thermolysis of a transition metal cluster complex containing these ligands usually results in the formation of products featuring highly coordinated acetylide and phosphido ligands.[7–11] Examples of polyyne ligand formation *via* coupling of smaller acetylide fragments derived from phosphinoacetylenes include the dimerisation of $[Fe_2(\mu\text{-}\eta^1,\eta^2\text{-}C_2Ph)(\mu\text{-}PPh_2)(CO)_6]$ to give $[Fe_4(\mu_4\text{-}PhC_4Ph)(\mu\text{-}PPh_2)_2(CO)_8]$,[2] and the analogous reaction of $[Ru_2(\mu\text{-}\eta^1,\eta^2\text{-}C_2Bu^t)(\mu\text{-}PPh_2)(CO)_6]$ which gives the diyne complex $[Ru_4(\mu_4\text{-}Bu^tC_4Bu^t)(\mu\text{-}PPh_2)_2(CO)_8]$ *via* the isolable tetrametallic intermediate $[Ru_4(\mu\text{-}PPh_2)_2(\mu\text{-}C_2Bu^t)_2(CO)_9]$.[3] These reactions are sensitive to the substituents on the acetylide ligand, as demonstrated by thermolysis of $[Ru_2(\mu\text{-}\eta^1,\eta^2\text{-}C_2Ph)(\mu\text{-}PPh_2)(CO)_6]$ which, in contrast to the reactions of the analogous Bu^t complex, gives products derived from head-to-tail coupling of the unsaturated hydrocarbon groups and P–C bond formation.[12]

In the bis(phosphinoalkyne) complexes $[Ru_3(CO)_{10}(Ph_2PC{\equiv}CR)_2]$ the phosphine ligands are expected to occupy coordination sites on adjacent ruthenium atoms with the uncoordinated alkyne substituents held proximate to the metals and to one another. By analogy with related *cis* bis(phosphinoalkyne) complexes of Pt(II)[13] these stereochemical features might be expected to enhance intramolecular alkyne coupling. Consequently, $[Ru_3(CO)_{10}(Ph_2PC{\equiv}CR)_2]$ complexes represent attractive and versatile starting materials for the exploration of acetylide–acetylide and acetylide–alkyne coupling reactions. We describe herein the thermolysis reactions of the disubstituted phosphinoalkyne clusters $[Ru_3(Ph_2PC{\equiv}CR)_2(CO)_{10}]$ (R = Ph, Bu^t) which generate several new acetylide clusters as well as products derived from acetylide–acetylide and acetylide–alkyne coupling.

Results and discussion

Reactions of $[Ru_3(CO)_{12}]$ with the readily available alkynes $Ph_2PC{\equiv}CR$ (R = Bu^t, Ph) in the presence of $[NBu_4]F$ (commercial solution in thf containing 5% water) afforded the disubstituted clusters $[Ru_3(CO)_{10}(Ph_2PC{\equiv}CR)_2]$ (R = Bu^t, **1a**; Ph, **1b**) in *ca.* 60% yields, following chromatographic separation from small amounts of $[Ru_3(CO)_{12-n}(Ph_2PC{\equiv}CR)_n]$ (n = 1, 3) and crystallisation. Lavigne and his colleagues have thoroughly investigated halide ions and other anions as catalysts for carbonyl substitution reactions with various phosphines and alkynes and given this previous work little more needs be said about the present examples.[14]

However, while offering an element of synthetic simplicity, in that the fluoride catalysed reactions can be carried out in air without the exclusion of moisture, the relatively low selectivity of the fluoride ion catalyst suggested that $[Ru_3(CO)_{10}(Ph_2PC{\equiv}CBu^t)(Ph_2PC{\equiv}CPh)]$ (**1c**), which contains two different phosphine ligands, would be better prepared by reaction of $[Ru_3(CO)_{11}(Ph_2PC{\equiv}CBu^t)]$[15] with $Ph_2PC{\equiv}CPh$ in the presence of $Na[Ph_2CO]$.[16] Using this route, **1c** was isolated in good yield.

The complexes **1a**–**c** were readily characterised by spectroscopic and microanalytical methods. In each case the IR spectrum contained a ν(CO) pattern typical of an $Ru_3(CO)_{10}L_2$ species, and doublets in the ^{31}P NMR spectra consistent with the presence of two coordinated phosphine ligands [**1a**, δ_P 4.07 (J_{PP} = 28 Hz); **1b**, δ_P 6.63 (J_{PP} = 82 Hz); **1c**, δ_P 6.25, 4.12 (J_{PP} = 20 Hz)]. Clusters **1a** and **1b** also gave a $\nu(C{\equiv}C)$ band near 2100 cm^{-1}. Mass spectra were obtained using fast atom bombardment (FAB) or atmospheric pressure chemical ionisation (APCI) methods and featured fragment ions derived from the sequential loss of CO ligands in each case. The molecular ion of **1a** was also observed by FAB-MS.

The solid-state structures of several phosphine and phosphite derivatives of general form $[Ru_3(CO)_{10}(L)_2]$ [L = PPh_3, $PPh(OMe)_2$, $P(OCH_2CF_3)_3$] have been determined.[17] In each case the clusters consist of a triangular Ru_3 core with the PR_3 ligands occupying equatorial positions on adjacent metal

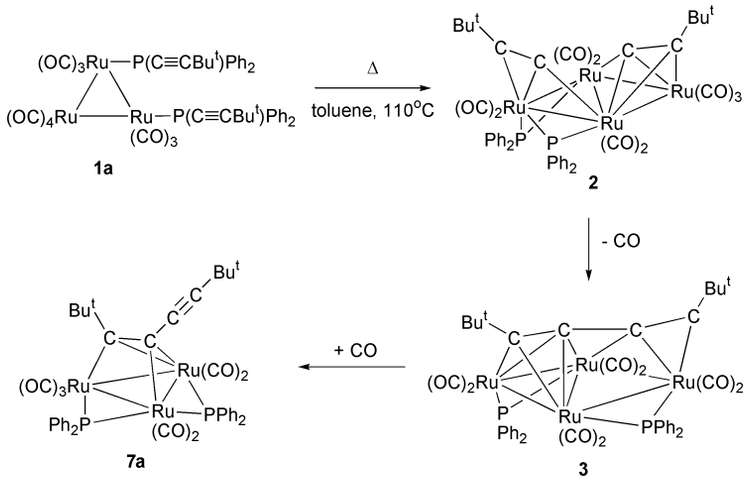

Scheme 1

atoms, approximately *trans* to each other through the Ru–Ru vector. The structure of **1a** was determined by single crystal X-ray diffraction methods (Fig. 1), and showed that the

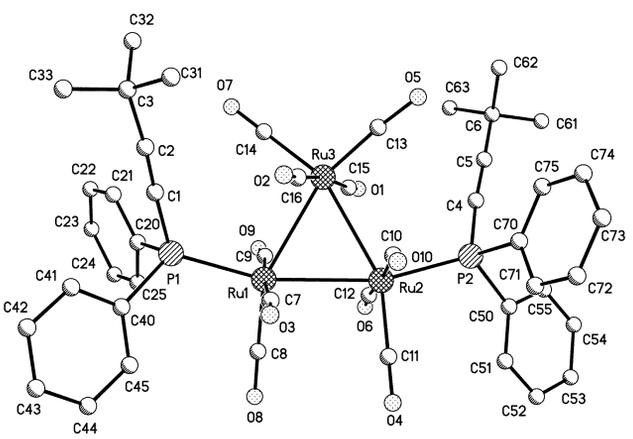

Fig. 1 Molecular structure of $[Ru_3(CO)_{10}(Ph_2PC{\equiv}CBu^t)_2]$ (**1a**) with hydrogen atoms omitted for clarity. Atoms are represented by spheres of arbitrary radii.

compound crystallises in space group *P*2(1), with the following unit cell parameters at 120 K: a = 9.493(4), b = 9.520(4), c = 25.187(11) Å, β = 96.19(1)°. The results confirmed the expected geometry but the low precision of the data, a consequence of the poor quality of the crystals, precludes detailed discussion of the results and comparisons with other $[Ru_3(CO)_{10}\mathbf{L}_2]$ species. Suffice it to say that the phosphine ligands in **1a** are coordinated at equatorial sites on two different metal centres, with the usual *trans* configuration relative to each other. Since these groups are free to rotate about the Ru–P bond, the acetylide moieties in the solid state are located in positions determined by both intramolecular interactions with the adjacent carbonyl ligands and crystal packing effects. The ligands around Ru(1) and Ru(2) are found in a staggered configuration with respect to the Ru(1)–Ru(2) bond.

Cluster **1a** underwent a series of fragmentation/condensation reactions upon thermolysis in toluene to give a mixture of the known tetraruthenium clusters $[Ru_4(\mu_3\text{-}\eta^1,\eta^2\text{-}C_2Bu^t)(\mu_2\text{-}\eta^1,\eta^2\text{-}C_2Bu^t)(\mu\text{-}PPh_2)_2(CO)_9]$ (**2**) and $[Ru_4(\mu_4\text{-}Bu^tC_4Bu^t)(\mu\text{-}PPh_2)_2(CO)_8]$ (**3**).[3] Prolonged thermolysis (7 h) resulted in the conversion of **2** to **3** *via* loss of a carbonyl ligand and a facile C–C bond forming reaction, and crystallisation of the reaction mixture afforded pure samples of the diyne cluster **3**. It has been demonstrated previously that treatment of **3** with CO (1 atm, 80 °C) results in elimination of an $Ru(CO)_n$ fragment and formation of the trinuclear diyne cluster $[Ru_3(\mu_3\text{-}Bu^tC_2C{\equiv}CBu^t)(\mu\text{-}PPh_2)_2(CO)_7]$ (**7a**) (Scheme 1).[3]

Under less vigorous conditions (hexane, 67 °C), **1a** gave the crimson coloured hexacarbonyl cluster $[Ru_3(\mu\text{-}\eta^1,\eta^2\text{-}C{\equiv}CBu^t)_2(\mu\text{-}PPh_2)_2(CO)_6]$ (**4**) (78 %) (Scheme 2). The structure of the

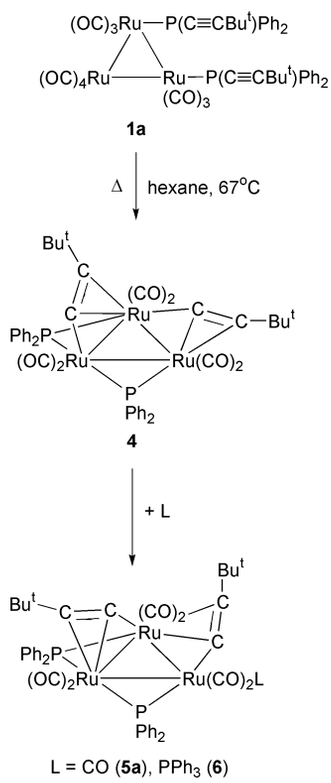

Scheme 2

product was inferred from the spectroscopic data and confirmed by a single crystal X-ray diffraction study (see below). Only terminal carbonyl ν(CO) bands were observed in the IR spectrum, while two resonances in the ^{1}H NMR spectrum (δ_H 0.84, 1.25) indicated the presence of two non- equivalent Bu^t groups. The FAB–MS of **4** contained the molecular ion at *m*/*z* 1004 and fragment ions derived from the sequential loss of six carbonyl ligands.

The structure of **4** (Fig. 2, Tables 1 and 2) revealed a triangle of ruthenium atoms [Ru(1,2) 3.219(5); Ru(1,3) 3.0081(5); Ru(2,3) 2.9044(5) Å], with each metal centre bearing two terminal carbonyl ligands. The shortest edge of the metal triangle [Ru(2)–Ru(3)] is bridged by both a μ-PPh_2 and a μ-η^1,η^2-C≡CR ligand, while the other edges are bridged by either a diphenylphosphido [Ru(1)–Ru(2)] or an acetylide [Ru(1)–Ru(3)] ligand. The acetylide ligands are found on the same face of the Ru_3

Table 1 Crystallographic details for complexes **4**, **5a**, **5b**, **5c**, **6**, **7c** and **8**

	4	**5a**	**5b**	**5c**	**6**	**7c**	**8**
Formula	$Ru_3P_2O_6C_{42}H_{38}$	$Ru_3P_2O_7C_{43}H_{38}$	$Ru_3P_2O_7C_{47}H_{30}$	$Ru_3P_2O_7C_{45}H_{34}$	$Ru_3P_3O_6C_{60}H_{53}\cdot CH_2Cl_2$	$Ru_3P_2O_7C_{45}H_{34}$	$Ru_3P_2O_8C_{48}H_{30}\cdot CHCl_3$
M	1003.87	1031.88	1071.86	1051.87	1351.07	1051.87	1219.24
Crystal system	Monoclinic	Monoclinic	Triclinic	Triclinic	Triclinic	Triclinic	Triclinic
Space group	$C2/c$	$P2_1/c$	$P\bar{1}$	$P\bar{1}$	$P\bar{1}$	$P\bar{1}$	$P\bar{1}$
a/Å	19.4209(14)	20.2682(10)	11.1720(5)	12.7431(6)	12.0485(5)	14.8147(8)	12.574(3)
b/Å	9.4333(7)	11.0110(5)	13.2256(6)	12.7649(6)	12.9634(6)	15.4012(9)	12.941(3)
c/Å	44.914(3)	20.1026(10)	15.5535(7)	16.5142(7)	20.4824(9)	19.3937(11)	15.380(3)
α/°	90	90	80.40(1)	68.47(1)	72.42(1)	90.69(1)	88.28(1)
β/°	99.42(1)	103.12(1)	70.17(1)	75.54(1)	87.32(1)	104.60(1)	87.37(1)
γ/°	90	90	89.39(1)	61.19(1)	89.12(1)	91.55(1)	71.98(1)
V/Å^3	8117(1)	4369.2(4)	2129.0(2)	2180.7(2)	3046.4(2)	4279.7(4)	2377.0(9)
T/K	173(2)	295(2)	173(2)	173(2)	173(2)	173(2)	100(2)
Z	8	4	2	2	2	4	2
μ/mm^{-1}	1.226	1.143	1.177	1.147	0.948	1.169	1.230
Unique data	36640	49056	25414	26030	24040	51171	31655
Observed data	10344	11306	10924	11214	10601	22012	11684
$R1$, $wR2$, $[I > 2\sigma(I)]$	0.0542, 0.1017	0.0450, 0.1069	0.0386, 0.0840	0.0317, 0.0674	0.0522, 0.1357	0.0417, 0.0771	0.0245, 0.0518

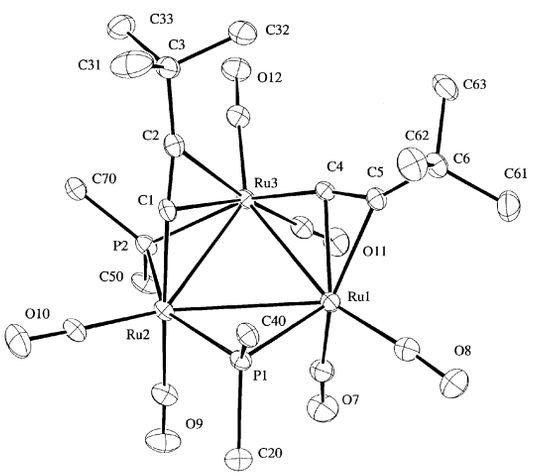

Fig. 2 Molecular structure of $[Ru_3(\mu\text{-}\eta^1,\eta^2\text{-}C{\equiv}CBu^t)_2(\mu\text{-}PPh_2)_2(CO)_6]$ (**4**). For clarity in this and some subsequent structures only the *ipso* carbon atoms of the PPh_2 aromatic groups are shown and all hydrogen atoms have been omitted.

triangle and are oriented in such a way as to minimise steric interactions between the bulky Bu^t head groups, while the phosphido ligands lie on opposite sides of the Ru_3 plane. Ru(1) appears to be coordinatively unsaturated, and adopts roughly square pyramidal geometry. It is likely that it is this site to which an additional ligand is attached upon reaction with CO or PPh_3 (*vide infra*).

The $\mu\text{-}\eta^1,\eta^2$ edge-bridging acetylide ligands are similar in structure to those in the electron-precise species $[Ru_2(\mu\text{-}\eta^1,\eta^2\text{-}C{\equiv}CBu^t)(\mu\text{-}PPh_2)(CO)_6]$[9] and $[Ru_3(\mu\text{-}\eta^1\text{-}C{\equiv}CBu^t)(\mu\text{-}\eta^1,\eta^2\text{-}C{\equiv}CBu^t)(\mu\text{-}PPh_2)_2(Ph_2PC{\equiv}CBu^t)(CO)_6]$.[10] In **4**, these ligands display a considerable deviation from linearity [Ru(2)–C(1)–C(2) 165.7(4), C(1)–C(2)–C(3) 162.4(5), Ru(3)–C(4)–C(5) 168.6(4), C(4)–C(5)–C(6) 149.0(4)°] and relatively long C–C separations [C(1)–C(2) 1.224(6) Å C(4)–C(5) 1.253(6) Å] due to the η^2 interactions with Ru(1) and Ru(3).

The σ-bonds between Ru(2) and C(1) [2.045(4) Å] and Ru(3) and C(4) [2.017(4) Å] are complemented by longer π-bonds to Ru(1) [Ru(1)–C(4, 5) 2.152(4), 2.217(4) Å] and Ru(3) [Ru(3)–C(1, 2) 2.323(4), 2.512(4) Å] and again these parameters are similar to those in $[Ru_2(\mu\text{-}\eta^1,\eta^2\text{-}C{\equiv}CBu^t)(\mu\text{-}PPh_2)(CO)_6]$ [2.044(3), 2.285(3), 2.417(3) Å].

If the acetylide ligands are regarded as conventional three-electron donors, **4** is an electron precise (48-electron) species. Cluster **4** was inert towards further pyrolytic reaction and could be recovered unchanged following thermolysis in toluene (24 h, 110 °C). This experiment clearly demonstrated that **4** was not an intermediate in the formation of **2**, and hence the diyne clusters **3** and **7a**. Ligand addition to the metal framework of **4** occurred readily, and treatment with carbon monoxide (r.t., 1 atm) or PPh_3 gave the yellow, electron rich (50-electron) clusters $[Ru_3(\mu\text{-}\eta^1,\eta^2\text{-}C{\equiv}CBu^t)_2(\mu\text{-}PPh_2)_2(CO)_7]$ (**5a**) and $[Ru_3(\mu\text{-}\eta^1,\eta^2\text{-}C{\equiv}CBu^t)_2(\mu\text{-}PPh_2)_2(PPh_3)(CO)_6]$ (**6**), respectively, in high yield (Scheme 2). The facile addition of the seventh CO ligand was readily reversed, and gentle warming of a solution of **5a** in thf or hexane afforded **4**. This cycle of CO addition and elimination was performed many times with no significant loss of material. Attempts to crystallise **4** from solutions containing methanol resulted in discolouration of the solution and deposition of yellow crystals of **5a**, presumably formed by an intermolecular CO abstraction process promoted by the polar solvent.

The IR spectra of **5a** and **6** contain ν(CO) patterns between 1941 and 2075 cm^{-1}, characteristic of all terminal carbonyl ligands. The ^{1}H NMR spectrum of **5a** indicated the presence of a second isomer in solution, with the major Bu^t signals shadowed by a second set of resonances (*ca.* 1 : 0.05; δ_H 0.082, 1.525). The well-known "windscreen-wiper" fluxional processes of one (or both) edge-bridging acetylide ligands probably relate the isomers (Scheme 3), which are in a slow exchange limit at

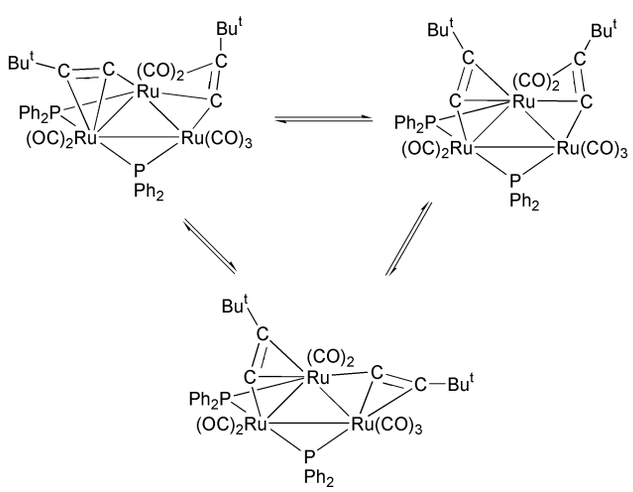

Scheme 3

room temperature.[9,18] At −60 °C (CD_2Cl_2) the motion is frozen out, and only a single isomer can be detected. The diphenylphosphido ligands in the major isomer of **5a** gave a pair of doublets in the ^{31}P NMR spectrum [δ 155.65, 144.19 (J_{PP} = 156 Hz)]. In the case of **6**, a sharp singlet in the ^{31}P NMR spectrum at δ 41.52 was observed in addition to the two

Table 2 Selected bond lengths (Å) and angles (°) for **4**, **5a**, **5b**, **5c** and **6**

	4	**5a**	**5b**	**5c**	**6**
Ru(1)–Ru(2)	3.219(5)	3.1422(5)	3.2832(3)	3.0594(3)	3.1004(5)
Ru(1)–Ru(3)	3.0081(5)	3.1467(4)	3.0583(3)	3.1859(3)	3.1903(6)
Ru(2)–Ru(3)	2.9044(5)	2.9120(12)	2.9415(3)	2.9716(3)	2.9241(6)
Ru(1)–C(4)	2.152(4)	2.052(4)	2.042(3)	2.050(3)	2.038(5)
Ru(2)–C(1)	2.045(4)	2.261(4)	2.304(2)	2.047(2)	2.292(6)
Ru(3)–C(1)	2.323(4)	2.105(5)	2.053(3)	2.321(2)	2.093(5)
Ru(3)–C(2)	2.512(4)	2.795(4) [for Ru(3) read Ru(2)]	2.576(2) [for Ru(3) read Ru(2)]	2.6767(2)	2.815(5) [for Ru(3) read Ru(2)]
Ru(3)–C(4)	2.017(4)	2.278(4)	2.282(3) [for Ru(3) read Ru(2)]	2.279(2)	2.314(4)
Ru(3)–C(5)	2.217(4) [for Ru(3) read Ru(1)]	2.436(4)	2.409(3) [for Ru(3) read Ru(2)]	2.426(3)	2.432(5)
C(1)–C(2)	1.224(6)	1.177(6)	1.210(4)	1.218(3)	1.183(7)
C(4)–C(5)	1.253(6)	1.226(6)	1.228(4)	1.230(4)	1.251(7)
P(1)–Ru(1)	2.292(1)	2.381(1)	2.3576(7)	2.3704(6)	2.409(1)
P(1)–Ru(2)	2.326(1)	2.348(1)	2.3473(7) [for Ru(2) read Ru(3)]	2.3283(6)	2.358(1)
P(2)–Ru(2)	2.350(1)	2.351(1)	2.3296(7)	2.3422(6)	2.340(1)
P(2)–Ru(3)	2.362(1)	2.310(1)	2.3473(7)	2.3235(7)	2.310(1)
Ru(1)–C(4)–C(5)	168.6(4) [for Ru(1) read Ru(3)]	174.0(4)	176.7(2)	170.7(2)	173.1(4)
C(4)–C(5)–C(6)	149.0(4)	161.7(5)	154.4(3) [for C(6) read C(60)]	159.7(4)	158.3(5)
Ru(2)–C(1)–C(2)	165.7(4)	167.2(4) [for Ru(2) read Ru(3)]	171.2(2) [for Ru(2) read Ru(3)]	173.2(2)	164.9(5) [for Ru(2) read Ru(3)]
C(1)–C(2)–C(3)	162.4(5)	170.7(6)	167.3(3) [for C(3) read C(30)]	170.0(3) [for C(3) read C(30)]	170.2(7)
Ru(1)–Ru(2)–Ru(3)		62.50(1)		63.76(1)	63.87(1)
Ru(2)–Ru(3)–Ru(1)	65.89(1)	62.34(1)	66.32(1)		
Ru(3)–Ru(1)–Ru(2)		55.17(1)			
Ru(1)–P(1)–Ru(2)	88.30(4)	83.28(4)	81.49(2) [for Ru(2) read Ru(3)]	81.24(2)	81.13(4)
Ru(2)–P(2)–Ru(3)	76.12(4)	77.32(4)	77.94(2)	79.12(2)	77.92(4)

doublets associated with the edge-bridging phosphido ligands [δ 158.22, 105.46 (J_{PP} = 142 Hz)], and assigned to the PPh_3 ligand. FAB–MS contained the expected molecular ions, which fragmented by loss of carbonyl ligands in each case.

An ORTEP plot of a molecule of **5a** is illustrated in Fig. 3.

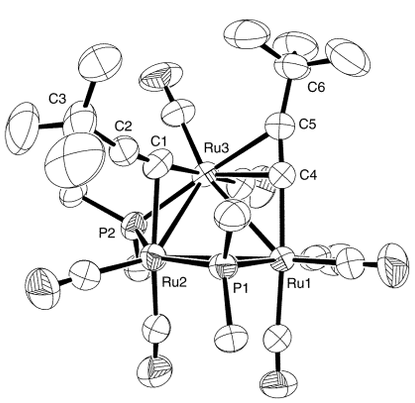

Fig. 3 The molecular structure of $[Ru_3(\mu\text{-}\eta^1,\eta^2\text{-}C{\equiv}CBu^t)_2(\mu\text{-}PPh_2)_2(CO)_7]$ (**5a**).

The three ruthenium atoms which comprise the metal core are arranged as an almost isosceles triangle [Ru(1, 2) 3.1422(5); Ru(1, 3) 3.1467(4); Ru(2, 3) 2.9120(12) Å]. The metal centres Ru(2) and Ru(3) each bear two terminal carbonyl ligands, while Ru(1) carries three of these ligands. The Ru(1)–Ru(3) and Ru(2)–Ru(3) bonds are bridged by acetylide ligands, while diphenylphosphido ligands are found bridging the Ru(1)–Ru(2) and Ru(2)–Ru(3) edges. As was found for **4**, the phosphido ligands in **5a** are located above and below the plane of the Ru_3 core, and the acetylide ligands, which lie on the same side of the cluster face as P(1), are arranged so as to minimise steric interactions between the Bu^t head groups. While the pattern of two long and one normal M–M bonds is common for electron-rich clusters with triangular M_3 cores,[19] the contraction of the Ru(2)–Ru(3) bond length relative to the other Ru–Ru separations in this cluster may be an artifact introduced by the two bridging ligands along this edge.

The metrical parameters of the C(4)≡C(5)Bu^t ligand (Table 2) are comparable with those described for the $\mu\text{-}\eta^1$, η^2 edge bridging ligands in **4** and the other examples cited above. The bend-back angles at C(4) and C(5) are 6.0(4) and 18.3(5)°, respectively. The acetylide ligand is coordinated in σ-fashion through C(4) to Ru(1) [Ru(1)–C(4) 2.052(4) Å] and π-coordinated to Ru(3) [Ru(3)–C(4, 5) 2.278(4), 2.436(4) Å; C(4)–C(5) 1.226(6) Å]. In contrast, the C(1)≡C(2)Bu^t fragment displays characteristics of a weaker π-bonding interaction with Ru(2) and a significant degree of $\mu_2\text{-}\eta^1$ character. Critical structural features include the short C(1)≡C(2) bond length [1.177(6) Å], which is more in keeping with an un-coordinated acetylene, and the long Ru(2)–C(2) bond length [2.795(4) Å]. The carbon centre C(1) makes contacts with both Ru(2) [2.261(4) Å] and Ru(3) [2.105(5) Å]. Nevertheless, it is not appropriate to describe the bonding of this ligand without a degree of π-bonding to Ru(2), as attested by the C(1)–C(2)–C(3) bond angle [170.7(6)°].

Table 3 Changes in metal–metal and metal–acetylide bond lengths in clusters **4**, **5a**, and **6**

	4	**5a**	**6**
Ru–Ru (av)	3.064	3.067	3.071
Ru–acetylide			
Ligand 1 (μ-PPh_2 edge)			
Ru^{σ}–C_{α}	2.045(4)	2.105(5)	2.093(4)
Ru^{π}–C_{α}	2.323(4) ⎫ av	2.261(4) ⎫ av	2.292 ⎫ av
Ru^{π}–C_{β}	2.512(4) ⎭ 2.418 Å	2.795(4) ⎭ 2.528 Å	2.815 ⎭ 2.868 Å
Ligand 2			
Ru^{σ}–C_{α}	2.017(4)	2.052(4)	2.038(4)
Ru^{π}–C_{α}	2.152(4) ⎫ av	2.278(4) ⎫ av	2.314(4) ⎫ av
Ru^{π}–C_{β}	2.217(4) ⎭ 2.185 Å	2.436(4) ⎭ 2.357 Å	2.432(4) ⎭ 2.373 Å
Ru–P			
Ru–P(2)(μ-C_2R side)	2.350(1) ⎫ av	2.381(1) ⎫ av	2.409(1) ⎫ av
	2.302(2) ⎭ 2.356 Å	2.348(1) ⎭ 2.364 Å	2.358(1) ⎭ 2.383 Å
Ru–P(1)(no-C_2R)	2.292(1) ⎫ av	2.351(1) ⎫ av	2.340(1) ⎫ av
	2.326(1) ⎭ 2.309 Å	2.310(1) ⎭ 2.331 Å	2.310(1) ⎭ 2.325 Å

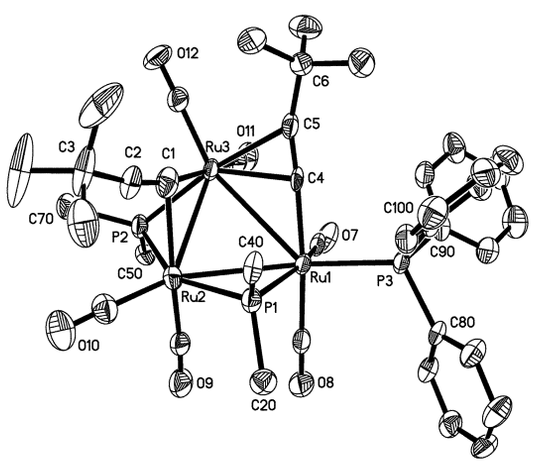

Fig. 4 The molecular structure of $[Ru_3(\mu\text{-}\eta^1,\eta^2\text{-}C{\equiv}CBu^t)_2(\mu\text{-}PPh_2)_2(PPh_3)(CO)_6]$ (**6**).

An ORTEP plot of a molecule of **6** is given in Fig. 4. The general arrangement of metal centres, acetylide and diphenylphosphido ligands is similar to that of the heptacarbonyl complex **5a**. The triangular metal core [Ru(1)–Ru(2) 3.1004(5), Ru(1)–Ru(3) 3.1903(6), Ru(2)–Ru(3) 2.9241(6) Å] supports two carbonyl ligands per metal centre. A PPh_3 ligand is coordinated to Ru(1), occupying the position *trans* to Ru(2). The acetylide ligands are asymmetrically bonded to the metal framework, and display geometries similar to those in **5a**. The structural parameters of the C(1)≡C(2)Bu^t ligand [C(1)–C(2) 1.183 Å, Ru(3)–C(1) 2.093(5) Å, Ru(2)–C(1) 2.292(6) Å, Ru(2)–C(2) 2.815(5) Å, Ru(3)–C(1)–C(2) 164.9(5), C(1)–C(2)–C(3) 170.2(7) °] are consistent with a weak π-interaction with Ru(2). The C(4)≡C(5)Bu^t ligand is bonded to Ru(1) and Ru(3) in conventional $\mu\text{-}\eta^1,\eta^2$ fashion [C(4)–C(5) 1.251(7) Å, Ru(1)–C(4) 2.038(5) Å, Ru(3)–C(4) 2.314(4), Ru(3)–C(5) 2.432(5) Å, C(4)–C(5)–C(6) 158.3(5) °] (Table 2).

A comparison of Ru–Ru, Ru–C and Ru–P bond lengths in clusters **4**, **5a** and **6** reveals several features which may reflect the additional electron density associated with the conversion of electron precise (48e) **4** to the electron rich clusters (50e) **5a** and **6**. For ease of reference these changes are summarised in Table 3. Somewhat surprisingly the change in electron count is relieved not by a significant expansion of the Ru_3 framework (the average Ru–Ru bond length increases only from 3.064 Å in **4** to 3.067 Å in **5a** to 3.071 Å in **6**) but principally by a decrease in the strength of the σ- and π-components of bonding of the acetylides to the metal framework. Thus for the acetylide ligand which bridges the same [Ru(2)–Ru(3)] edge as the μ-PPh_2 ligand [P(2)] the Ru^{σ}–C_{α} (acetylide) distance increases significantly from 2.045(4) Å in **4** to 2.105(5) Å in **5a** and 2.093(4) Å in **6**. A similar but smaller increase is evident in the Ru^{σ}–C_{α} bond lengths for the acetylide bridging the Ru(1)–Ru(3) edge [2.017(4) Å in **4** to 2.052(4) Å in **5a** and 2.038(4) Å in **6**]. The metal–acetylide π-interactions are also weakened from **4** to **5a** and **6** with the average Ru^{π}–C_{α} and Ru^{π}–C_{β} distances increasing significantly, particularly for the acetylide ligand bridging the Ru(2)–Ru(3) (μ-PPh_2) edge [Ru^{π}–C 2.418 Å, **4**; 2.528 Å, **5a**; 2.868 Å, **6**]. Similar trends are evident in the average Ru–PPh_2 distances from **4** to **5a** and **6** although the magnitude of the increases is less. Following on the above observations it is interesting to note that the closely related electron-rich bis(acetylide) cluster $[Os_3(\mu\text{-}\eta^1,\eta^2\text{-}C{\equiv}CPr^i)_2(\mu\text{-}PPh_2)_2(CO)_7]$ displays an expanded M_3 core, but in this case both acetylide ligands are conventionally bonded in $\mu\text{-}\eta^1,\eta^2$ fashion.[11] It is also interesting to consider the structures of the electron-precise complexes $[Ru_3(\mu\text{-}\eta^1,\eta^2\text{-}C{\equiv}CBu^t)(\mu\text{-}\eta^1\text{-}C{\equiv}CBu^t)(\mu\text{-}PPh_2)_2(Ph_2PC{\equiv}CBu^t)(CO)_6]$,[10] which features a symmetrical $\mu_2\text{-}\eta^1$ acetylide ligand, and the osmium cluster $[Os_3(\mu\text{-}\eta^1,\eta^2\text{-}C{\equiv}CPh)(\mu\text{-}\eta^1\text{-}C{\equiv}CPh)(\mu\text{-}PPh_2)_2(NHEt_2)_2(CO)_6]$ which contains a non-bridging η^1-acetylide ligand.[11] Both of these compounds can be derived formally from net addition of a two electron ligand to a 48-e $[M_3(\mu\text{-}\eta^1,\eta^2\text{-}C{\equiv}CR)_2(\mu\text{-}PPh_2)_2(CO)_6]$ framework with the extra pair of electrons compensated by the conversion of a 3e donating $\eta^1,\eta^2\text{-}C_2R$ ligand to a 1e donating η^1 mode.

Thermolysis of **1b** in refluxing thf (90 min) gave a mixture of the yellow 50-e cluster $[Ru_3(\mu\text{-}\eta^1,\eta^2\text{-}C{\equiv}CPh)_2(\mu\text{-}PPh_2)_2(CO)_7]$ (**5b**, 20 %), the known 48-e trimetallic red diyne cluster $[Ru_3(\mu_3\text{-}PhC_2C{\equiv}CPh)(\mu\text{-}PPh_2)_2(CO)_7]$ (**7b**, 5%),[20] and the novel complex $\{Ru_2[PhCC(PPh_2)CCPh](CO)_5\}(\mu\text{-}PPh_2)[Ru(CO)_3]$ (**8**, 39%) which were separated by preparative TLC (Scheme 4). In a separate experiment, **5b** was found to convert to **7b** rapidly and in high yield (>70%) upon thermolysis (1 h) in refluxing toluene.

Thermolysis of the mixed phosphine substituted cluster **1c** in refluxing thf (90 min) gave the electron rich 50-e cluster $[Ru_3(\mu\text{-}\eta^1,\eta^2\text{-}C{\equiv}CPh)(\mu\text{-}\eta^1,\eta^2\text{-}C{\equiv}CBu^t)(\mu\text{-}PPh_2)_2(CO)_7]$ (**5c**)

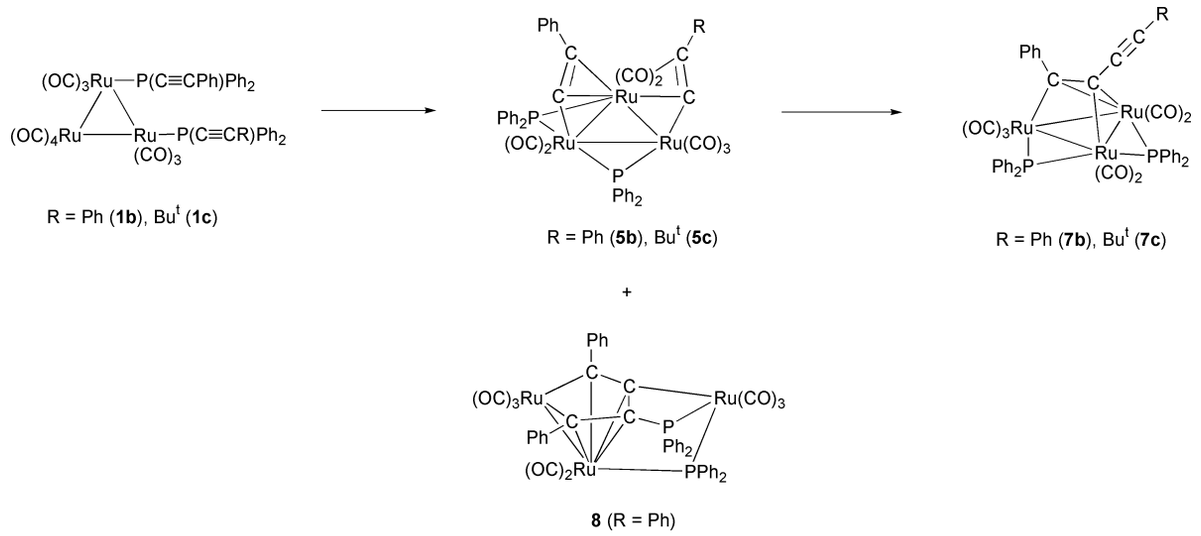

Scheme 4

(27%) together with the red diyne cluster $[Ru_3(\mu_3\text{-}PhC_2C{\equiv}CBu^t)(CO)_7(\mu\text{-}PPh_2)_2]$ (**7c**) (5%) and several other minor products which were not characterised (Scheme 4). Thermolysis of **1c** in refluxing toluene (110 °C, 3h) also afforded **5c** (20 %) and **7c** (20%). A separate experiment confirmed that **5c** converts to **7c** under these conditions and prolonged reaction (24 h) resulted in complete conversion of **1c** to **7c**, which was isolated in 30 % yield.

The ^{1}H NMR spectrum of **5b** was not especially informative, containing only a series of overlapping multiplets arising from the aromatic moieties. However the ν(CO) and ^{31}P NMR spectra of **5b** were very similar to those of **5a**. The IR spectrum of the heptacarbonyl cluster **5c** contained a ν(CO) band pattern similar to that of the other examples described above. The solution NMR data was consistent with the presence of two isomers of **5c**, with both ^{1}H [δ 1.07 (major); 0.02 (minor)] and ^{13}C [δ 32.66, 33.01 (major); 30.60, 30.16 (minor)] spectra showing two magnetically distinct Bu^t groups (*ca.* 1: 0.2) in solution. Microanalytical and FAB–MS data were in accord with the proposed structures, which were confirmed by X-ray methods.

The molecular structure of the bis(phenylacetylide) complex **5b** is given in Fig. 5. The triangular cluster core [Ru(1)–Ru(2)

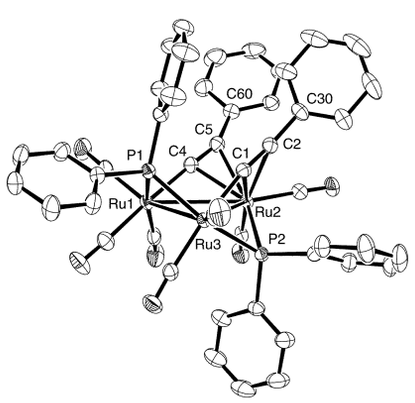

Fig. 5 The molecular structure of $[Ru_3(\mu\text{-}\eta^1,\eta^2\text{-}C{\equiv}CPh)_2(\mu\text{-}PPh_2)_2(CO)_7]$ (**5b**).

3.2832(3), Ru(1)–Ru(3) 3.0583(3), Ru(2)–Ru(3) 2.9415(3) Å] is the most expanded of the three compounds **5a** (Ru–Ru av 3.067 Å), **5b** (Ru–Ru av 3.094 Å) and **5c** (Ru–Ru av 3.072 Å) and carries two edge-bridging acetylide ligands, two bridging diphenylphosphido groups, and seven terminal carbonyl ligands. While the general arrangement of these ligands is similar to that of **5a**, both acetylide ligands in **5b** are coordinated in the η^2 mode to the same metal centre [Ru(2)]. The same ligand arrangement has been observed in the bis(isopropylacetylide) complex $[Os_3(\mu\text{-}\eta^1,\eta^2\text{-}C{\equiv}CPr^i)_2(\mu\text{-}PPh_2)_2(CO)_7]$,[11] suggesting that intramolecular steric factors between bulky *tert*-butyl substituents as in **5a** may play a role in determining the ligand arrangement adopted in the solid state.

The structural parameters of the two edge-bridging acetylide ligands are similar [Ru(1)–C(4) 2.042(3), Ru(3)–C(1) 2.053(3) Å, Ru(2)–C(1, 2, 4, 5) 2.304(2), 2.576(2), 2.282(3), 2.409(3) Å, Ru(1)–C(4)–C(5) 176.7(2), Ru(3)–C(1)–C(2) 171.2(2), C(1)–C(2)–C(30) 167.3(3), C(4)–C(5)–C(60) 154.4(3)°], and fall within the normal ranges.

The structure of **5c** (Fig. 6) is similar to that of **5b** (Tables 2

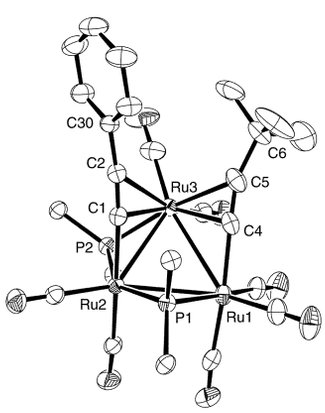

Fig. 6 The molecular structure of $[Ru_3(\mu\text{-}\eta^1,\eta^2\text{-}C{\equiv}CPh)(\mu\text{-}\eta^1,\eta^2\text{-}C{\equiv}CBu^t)(\mu\text{-}PPh_2)_2(CO)_7]$ (**5c**).

and 3). Within the triangular Ru_3 core the average Ru–Ru distance (3.072 Å) is virtually identical to that in **5a** (3.067 Å) and supports the familiar pattern of edge-bridging acetylide ligands, with both *tert*-butyl and phenyl acetylides η^2-coordinated to Ru(3). The acetylide ligands are distinguished by a more pronounced bend-back angle at C(5) [20.3(4)°] than C(2) [10.0(3)°], a longer acetylide bond length in the case of C(4)≡C(5) [1.230(4) Å] than C(1)≡C(2) [1.218(3) Å] and longer bonds between Ru(3) and C(1)≡C(2) [Ru(3)–C(1,2) 2.321(2), 2.676(2)] than C(4)≡C(5) [Ru(3)–C(4,5) 2.279(2), 2.426(3) Å]. A further point of interest is that the structural parameters for the coordinated C≡CBu^t ligand in **5c** are essentially identical to those in the analogous ligand in **5a**. When these observations are taken together, they suggest that bonding between Ru(3) and the *tert*-butyl substituted acetylide ligand is stronger than that between the same metal centre and the phenylacetylide group. This is perhaps an unexpected result in that a σ,π-bound

acetylide group bearing an electron withdrawing substituent such as a phenyl group might be expected to provide greater stabilisation of the electron rich cluster core in **5b**, **5c** *via* increased π-back donation from the metal centres. Indeed such a conclusion might be drawn from a comparison of **5a** and **5b** where the two phenylacetylide groups in **5b** appear to be more strongly π-bound. These results suggest that molecules **5a–c** are likely to have a soft and easily deformable potential energy surface such that relatively small changes in metal–metal and metal–hydrocarbyl bonding can significantly alter structural features.

Cluster **7b** has previously been prepared from the reaction of diphenylbutadiyne with the electron-rich cluster $[Ru_4(CO)_{13}(\mu\text{-}PPh_2)_2]$ *via* a facile fragmentation reaction,[20] and the corresponding $Bu^tC{\equiv}CC{\equiv}CBu^t$ complex (**7a**) is also known.[3] The spectroscopic properties of **7c** are similar to those of **7a**,**b** and the other related examples cited above and elsewhere,[3,20,21] with only terminal carbonyl ν(CO) bands observed in the IR spectrum and a FAB–MS containing the molecular ion, which fragmented by loss of carbonyl ligands. The ^{1}H NMR spectrum contained resonances arising from the Bu^t (δ 0.97) and aromatic protons in the expected ratio. The ^{13}C NMR spectrum contained resonances at δ_C 90.22 and 107.00 which were attributed to the carbon nuclei of the uncoordinated alkynyl moiety. The carbon nuclei of the cluster bound alkyne moiety could not be detected. While the spectroscopic data did not resolve the regiochemistry of the diyne ligand in **7c**, the solid state structure (Fig. 7) showed the $PhC{\equiv}CC{\equiv}CBu^t$ diyne ligand to be

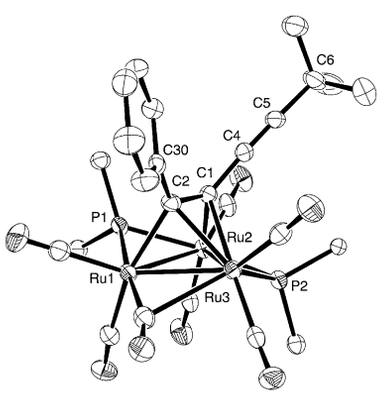

Fig. 7 The molecular structure of one of the independent molecules of $[Ru_3(\mu_3\text{-}\eta^2\text{-}PhC_2C{\equiv}CBu^t)(\mu\text{-}PPh_2)_2(CO)_6]$ (**7c**). Selected bond lengths (Å) and angles (°) for molecules 1/2: Ru(1)–Ru(2) 2.8870(5)/2.8793(5); Ru(1)–Ru(3) 2.7256(5)/2.7370(5); Ru(2)–Ru(3) 2.8446(5)/2.8121(5); Ru(1)–C(2) 2.154(4)/2.149(4); Ru(2)–C(1) 2.139(4)/2.138(4); Ru(3)–C(1) 2.298(4)/2.292(4); Ru(3)–C(2) 2.291(4)/2.285(4); Ru(1)–P(1) 2.370(1)/2.375(1); Ru(2)–P(1) 2.321(1)/2.317(1); Ru(2)–P(2) 2.319(1)/2.327(1); Ru(3)–P(2) 2.278(1)/2.276(1); C(1)–C(2) 1.386(6)/1.388(6); C(1)–C(4) 1.439(5)/1.435(6); C(4)–C(5) 1.188(5)/1.194(6); C(2)–C(30) 1.479(6)/1.500(6); C(5)–C(6) 1.474(6)/1.47(1); Ru(1)–Ru(2)–Ru(3) 56.78(1)/57.48(1); Ru(2)–Ru(3)–Ru(1) 62.39(1)/62.50(1); Ru(3)–Ru(1)–Ru(2) 60.82(1)/60.03(1); Ru(1)–P(1)–Ru(2) 75.96(3)/75.69(3); Ru(2)–P(2)–Ru(3) 76.45(4)/75.30(4); C(30)–C(2)–C(1) 125.3(4)/125.1(4); C(2)–C(1)–C(4) 126.1(4)/125.9(4); C(1)–C(4)–C(5) 174.4(4)/174.2(5); C(4)–C(5)–C(6) 178.7(5)/169.5(7).

coordinated through the PhC≡C moiety. Two independent molecules were contained in the asymmetric unit, essentially differing only in the degree of disorder in the Bu^t moiety. Since there are no structural distinctions of significance, the discussion below refers only to the least disordered molecule.

A molecule of **7c** is illustrated in Fig. 7, and clearly shows the $PhC{\equiv}CC{\equiv}CBu^t$ ligand coordinated to the triangular Ru_3 cluster. The three Ru–Ru bonds [Ru(1)–Ru(2) 2.8870(5), Ru(1)–Ru(3) 2.7256(5), Ru(2)–Ru(3) 2.8446(5) Å, av. 2.8191(5) Å] are somewhat longer than found in the related carbonyl cluster $[Ru_3(\mu_3\text{-}\eta^2\text{-}PhC_2C{\equiv}CPh)(\mu\text{-}CO)(CO)_9]$ (av 2.77_5 Å), but fall within the ranges associated with **7b**.[20] The other structural parameters are as expected, with the pendant C(4)≡C(5) moiety behaving as a typical alkyne [C(4)–C(5) 1.188(5) Å, C(1)–C(4)–C(5) 174.4(4), C(4)–C(5)–C(6) 178.7(5)°], and the C(1)–C(2) bond being rather elongated [1.386(6) Å]. The C(sp)–C(sp) bond which links the alkyne moieties is 1.439(5) Å and bend-back angles at C(1) and C(2) are 53.9° and 54.7°, respectively.

Cluster complexes formed by reactions with asymmetric $RC{\equiv}CC{\equiv}CR'$ diynes are generally present as 1 : 1 mixtures of the two regioisomers,[22] although some specificity has been demonstrated in the coordination of WCl_6 to $PhC{\equiv}CC{\equiv}CSiMe_3$,[23] and in very recent work,[24] which has been attributed to electronic effects. The regiochemistry observed in reactions of metallodiynyl complexes $[ML_n]C{\equiv}CC{\equiv}CR$ with other metal reagents appears to be governed by the steric influence of the ML_n fragment.[25] Remarkably, only one regio-isomer of **7c** was formed, and NMR investigations of both the crude reaction mixture and solutions of the isolated product failed to reveal the presence of the other regioisomer. In contrast to $[Os_3(\mu_3\text{-}PhC_2C{\equiv}CPh)(\mu\text{-}CO)(CO)_9]$ [22a] and $Ru_3(\mu_3\text{-}PhC_2C{\equiv}CPh)(\mu\text{-}CO)(CO)_7L_2$ (L = CO, L_2 = dppm) [26] which are thermally sensitive and give products derived from C–C bond cleavage, partial hydrogenation of the diyne ligand or cluster fragmentation upon heating, both **7b** and **7c** are inert to further thermal reactions. The resilience of **7** to fragmentation processes is attributed to the stabilising influence of the $\mu\text{-}PPh_2$ groups.

The different solid-state structures and thermal rearrangement pathways observed for the electron-rich heptacarbonyl complexes **5a** and **5b**,**c** prompt consideration of the steric and electronic factors which dictate the course of these reactions. It is clear from the room temperature NMR data that the acetylide ligands are confined to their respective Ru–Ru edges, and both **5a** and **5c** exist as two isomers in solution. However, given the asymmetry in the metal frameworks in the present examples, the NMR data cannot distinguish between a concerted fluxional process, in which both acetylide ligands maintain their respective orientation from a sequential exchange of the ligand positions (Scheme 3). Thus, while we favour a steric argument it is not possible to attribute the difference in reactivity to the alignment of the acetylide ligands at this time, as all three complexes **5a**,**b**,**c** *may* adopt a similar arrangement in solution.

The major product (*ca.* 40 %) isolated from the thermolysis of **1b** was the substituted ruthenole complex **8**. The IR spectrum featured an eight band ν(CO) pattern, while the FAB–MS contained an ion at *m*/*z* 1101 and fragment ions derived from the loss of eight carbonyl ligands. The ^{31}P NMR contained two doublets (J_{PP} = 11 Hz), indicative of a phosphine ligand (δ 16.48) and a phosphido ligand spanning two non-bonded metal centres (δ −77.89) [15,27] while the ^{13}C NMR spectrum contained eight resonances from the carbon nuclei of the carbonyl ligands. Cluster **8** was inert towards further thermolysis, and could be recovered intact following prolonged treatment in refluxing toluene, indicating that **8** was not an intermediate in the formation of **5b**, but rather originated from a different thermolytic reaction path. The molecular structure of this material was established by a single crystal X-ray diffraction study.

The X-ray structure of **8** (Fig. 8) revealed that the Ru_3 triangle in **1b** has fragmented to give a ruthenole-like structure, substituted at C(4) by a $Ru(CO)_3$ fragment. Only one of the phosphinoacetylene ligands in **1b** has undergone P–C bond cleavage and the resulting phosphido ligand spans the non-bonded metal centres Ru(2) and Ru(3) in asymmetric fashion [P(2)–Ru(2) 2.3665(7) Å, P(2)–Ru(3) 2.4633(7) Å, Ru(2)–P(2)–Ru(3) 98.24(2)°]. The $Ph_2P(1)$–C(1)–C(2)Ph chain is found intact. The Ru(1)–Ru(2) separation is 2.7413(3) Å, which is consistent with the range of values [2.734(3)–2.743(3) Å] found in similar complexes derived from alkynes.[28] The bond distances around the metallocyclopentadienyl ring system [Ru(1)–C(5) 2.128(2), Ru(1)–C(2) 2.079(2), C(1)–C(2) 1.426(3), C(1)–C(4) 1.459(3),

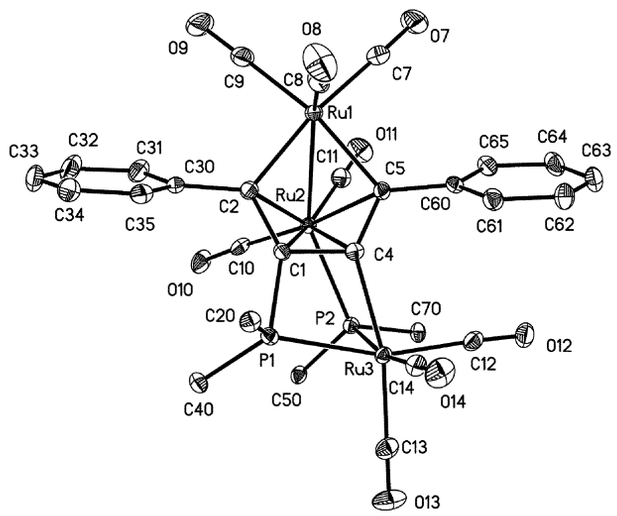

Fig. 8 The molecular structure of $\{Ru_2[\eta^1,\eta^1{:}\eta^2,\eta^2\text{-}PhCC(PPh_2)\text{-}CCPh](CO)_5\}(\mu\text{-}PPh_2)[Ru(CO)_3]$ (**8**). Selected bond lengths (Å) and angles (°): Ru(1)–Ru(2) 2.7593(6); Ru(2)–P(2) 2.3665(7); Ru(3)–P(1) 2.4150(8); Ru(3)–P(2) 2.4633(7); Ru(1)–C(2) 2.076(2); Ru(1)–C(5) 2.119(2); Ru(3)–C(4) 2.173(2); C(1)–C(2) 1.433(3); C(1)–C(4) 1.461(3); C(1)–P(1) 1.807(2); C(2)–C(30) 1.494(3); C(4)–C(5) 1.402(3); C(5)–C(60) 1.487(3); Ru(1)–Ru(2)–P(2) 144.59(2); Ru(2)–P(2)–Ru(3) 98.24(2); C(2)–Ru(1)–C(5) 80.13(8); Ru(1)–C(5)–C(4) 114.3(1); C(5)–C(4)–C(1) 114.5(2); C(4)–C(1)–C(2) 117.3(2); C(1)–C(2)–Ru(1) 113.1(1); C(1)–P(1)–Ru(3) 86.41(7); P(1)–Ru(3)–C(4) 65.28(6); Ru(3)–C(4)–C(1) 105.5(1).

C(4)–C(5) 1.401(3) Å] are normal, as are the bonds from the π-coordinated Ru(2) centre to the ruthenacyclopentadiene ring [2.180(2)–2.337(2) Å]. The coordination of P(1) to the pendant Ru(3) centre, which is also coordinated to C(4), results in rather distorted geometries at the formally sp^2 carbon centres C(1) and C(4) [C(2)–C(1)–P(1) 143.2(2), P(1)–C(1)–C(4) 98.3(2), C(1)–C(4)–Ru(3) 105.0(1), Ru(3)–C(4)–C(5) 138.4(2)°]. In this respect, the structure is not dissimilar to that reported for $[Ru_2\{\mu\text{-}2\eta^1,\eta^4,\mu\text{-}2\eta^1\text{-}PhCCCCPh[Ru_2(CO)_8]\}]$, in which an *exo* $Ru_2(CO)_8$ fragment is coordinated to a ruthenacyclopentadiene fragment.[26]

Complex **8** is unusual in that only one of the P–C bonds present in the precursor **1b** has undergone cleavage, and the resulting acetylide ligand fragment couples with the intact P–C≡C–moiety to afford the familiar Ru_2C_4 ruthenole fragment.[29] Indeed, **8** appears to be a unique example of a ruthenole complex by virtue of the phosphine substitution at C(1). The isolation of **8** from the thermal reaction of **1b** without the observation of any comparable products from the rearrangement of **1a** or **1c** provides another example of the sensitivity of acetylide coupling reactions to the nature of the acetylide substituents.

Experimental

General conditions

All reactions were carried out using standard Schlenk techniques under dry high-purity nitrogen. Solvents were dried and distilled prior to use. Preparative TLC was carried out on 20 × 20 cm glass plates coated with silica gel (Merck G_{254}, 0.5 mm thick). Literature methods were used to prepare $Ph_2PC{\equiv}CBu^t$ and $Ph_2PC{\equiv}CPh$.[30] Other reagents were purchased and used as received. IR spectra were recorded on a Nicolet Avatar spectrophotometer using solution cells fitted with CaF_2 windows. NMR spectra were obtained from solutions in $CDCl_3$ unless otherwise noted using Varian VXR-400 (^{1}H 399.97, ^{13}C 100.57, ^{31}P 161.1 MHz) or Bruker DRX-400 (^{1}H 400.13, ^{13}C 100.61, ^{31}P 162.05 MHz) spectrometers. FAB–MS were recorded on a JEOL AX505 mass spectrometer using Xe as the exciting gas, FAB gun voltage 6 kV, accelerating potential 3 kV using *m*-nitrobenzyl alcohol as a matrix. APCI–MS were collected on a Micromass LCT instrument.

Preparations

$[Ru_3(CO)_{10}(Ph_2PC{\equiv}CBu^t)_2]$ (1a). A 250ml Schlenk flask was charged with powdered $[Ru_3(CO)_{12}]$ (2.00 g, 3.13 mmol) and $Ph_2PC{\equiv}CBu^t$ (1.67 g, 6.28 mmol), and the solids dissolved in thf (100 ml). Treatment of the mixture with a solution of $[NBu_4]F$ (Aldrich, 1.0 M in thf–H_2O, 0.6 ml, 0.6 mmol) resulted in an immediate evolution of CO and a darkening of the colour of the solution from orange to dark red. The reaction mixture was stirred for 5 min, after which time TLC analysis and IR spectroscopy indicated complete consumption of the reagents. A small portion of silica gel was added to the reaction flask, and the solvent removed. The stained silica gel was added atop a silica gel column (hexane), and the reaction products eluted with a hexane–CH_2Cl_2 gradient. A minor orange band containing $[Ru_3(CO)_{11}(Ph_2PC{\equiv}CBu^t)]$ (0.20 g, 7 %) was eluted with 10% CH_2Cl_2, while the major dark red fraction eluted with 20% CH_2Cl_2. Crystallisation of this second band (CH_2Cl_2–MeOH) afforded $[Ru_3(CO)_{10}(Ph_2PC{\equiv}CBu^t)_2]$ (2.20 g, 63%) as dark red block-shaped crystals. IR (cyclohexane): ν(C≡C) 2165w; ν(CO) 2072w, 2044w, 2020s, 1995s(br) cm^{-1}. ^{31}P NMR: δ 4.07 (d, J_{PP} = 28 Hz). FAB–MS: 1117, $[M]^+$; 1005–837, $[M - nCO]^+$ (n = 4–10). $Ru_3P_2O_{10}C_{46}H_{38}$ requires C 49.51, H 3.43%. Found C 49.59, H 3.44%.

$[Ru_3(CO)_{10}(Ph_2PC{\equiv}CPh)_2]$ (1b). A similar procedure to that described for **1a** gave $[Ru_3(CO)_{10}(Ph_2PC{\equiv}CPh)_2]$ (60%). IR (cyclohexane): ν(C≡C) 2169w; ν(CO) 2073w, 2045w, 2021s, 1997s(br) cm^{-1}. ^{31}P NMR: δ 6.63 (d, J_{PP} = 82 Hz). APCI–MS: 1045–933 $[M - nCO]^+$ (n = 4–8). $Ru_3P_2O_{10}C_{50}H_{30}$ requires C 51.86, H 2.62%. Found C 52.09, H 2.80%.

$[Ru_3(CO)_{10}(Ph_2PC{\equiv}CPh)(Ph_2PC{\equiv}CBu^t)]$ (1c). A solution of $[Ru_3(CO)_{11}(Ph_2PC{\equiv}CBu^t)]$ (0.425 g, 0.484 mmol) and $Ph_2PC{\equiv}CPh$ (0.140 g, 0.489 mmol) in thf (40 ml) was treated with a solution of $Na[Ph_2CO]$ in thf dropwise until TLC and IR analysis showed complete conversion to **1c**. The solvent was removed and the resulting dark red residue purified by column chromatography on silica gel. Elution with a CH_2Cl_2 gradient (10–20%) in hexanes afforded a dark red band, which was concentrated to give **1c** (0.386 g, 70%). IR (cyclohexane): ν(CO) 2075m, 2023s, 2003sh, 1994w. ^{31}P NMR: δ 4.12 (d, J_{PP} = 20 Hz), 6.25 (d, J_{PP} = 20Hz). APCI–MS: 1025–941 $[M - nCO]^+$ (n = 4–7). $Ru_3P_2O_{10}C_{48}H_{34}$ requires C 50.75, H 3.02%. Found C 50.54, H 2.98%.

Pyrolysis of $[Ru_3(CO)_{10}(Ph_2PC{\equiv}CBu^t)_2]$ in toluene. A sample of $[Ru_3(CO)_{10}(Ph_2PC{\equiv}CBu^t)_2]$ (200 mg, 0.18 mmol) in toluene (15 ml) was heated at reflux point for 5 h. Removal of the solvent and crystallisation of the residue afforded a mixture of $[Ru_4(\mu\text{-}C_2Bu^t)_2(\mu\text{-}PPh_2)_2(CO)_9]$ (**2**) and $[Ru_4(Bu^tC_4Bu^t)(\mu\text{-}PPh_2)_2(CO)_8]$ (**3**) which were identified by the characteristic ν(CO) band patterns.[3] Purification by preparative TLC (CH_2Cl_2–hexane : 3/7) afforded one major orange band which gave $[Ru_4(\mu\text{-}C_2Bu^t)_2(\mu\text{-}PPh_2)_2(CO)_9]$ (70 mg, 32 %) following crystallisation (CH_2Cl_2–MeOH).

$[Ru_3(\mu\text{-}C_2Bu^t)_2(\mu\text{-}PPh_2)_2(CO)_6]$ (4). *Method 1.* A solution of **1a** (509 mg, 0.457 mmol) in hexane (40 ml) was heated at reflux for 3 h, during which time the solution darkened to blood red and IR analysis indicated complete consumption of the starting material (the band at 1996 cm^{-1} was followed). The solvent was allowed to evaporate and the residue crystallised (CH_2Cl_2–hexane, −18 °C) to afford dark red block-shaped crystals of $[Ru_3(\mu\text{-}C_2Bu^t)_2(\mu\text{-}PPh_2)_2(CO)_6]$ (**4**) suitable for X-ray analysis (358 mg, 78 %). IR: (cyclohexane) ν(CO) 2043s, 2018vs, 2001s, 1976vs, 1965s, 1951w, 1930vw cm^{-1}. ^{1}H NMR: 0.84, 1.25 (2 × s, 2 × 9H, 2 × Bu^t); 7.24–7.39, 7.57–7.64 (m, 20H,

Ph). FAB–MS: 1004, M^+; 977–837, $[M - nCO]^+$ (n = 1–6). $Ru_3P_2O_6C_{42}H_{38}$ requires C 50.15, H 3.78%. Found C 49.89, H 3.87%.

Method 2. A solution of **5a** (70 mg, 0.068 mmol) in hexane (15 ml) was heated at reflux for 12 h. During this time the initially yellow solution turned dark red. The solvent was allowed to evaporate and the resulting residue crystallised as above to afford **4** (60 mg, 88 %).

$[Ru_3(\mu\text{-}C_2Bu^t)_2(\mu\text{-}PPh_2)_2(CO)_7]$ (5a). A solution of **1a** (200 mg, 0.18 mmol) in thf (15 ml) was heated at reflux point for 1 h. After this time, the dark red solution containing **4** (by IR) was fitted with a CO purge and allowed to cool, which resulted in a lightening in colour of the reaction mixture. The solvent was removed, and the residue crystallised from CH_2Cl_2–MeOH to yield yellow crystals of $[Ru_3(\mu\text{-}C_2Bu^t)_2(\mu\text{-}PPh_2)_2(CO)_7]$ (**5a**) (120 mg, 64 %). IR (cyclohexane): 2075s, 2022vs, 2003m, 1961m cm^{-1}. ^1H NMR: (room temperature) δ 0.31, 1.43 (2 × s, 2 × 8H, 2 × Bu^t, isomer 1); 0.08, 1.53 (2 × s, 2 × 1H, 2 × Bu^t, isomer 2); 7.87–8.23 (m, 20H, Ph); ^{13}C NMR: δ 29.65, 29.84 (2 × s, 2 × CBu^t); 31.72, 32.60 (2 × s, 2 × $C(CH_3)_3$); 102.63 (d, J_{CP} = 8.7 Hz), 105.55 (d, J_{CP} = 9.2 Hz) (2 × C≡C); 127.05–142.09 (Ph); 193.42, 194.54, 195.47, 196.09, 198.16, 198.89, 200.38 (7 × CO). ^{31}P NMR: δ 144.18 (d, J_{PP} = 156 Hz); 155.67 (d, J_{PP} = 156 Hz). FAB–MS: 1031, $[M]^+$; 1003–835, $[M - nCO]^+$ (n = 1–7). $Ru_3P_2O_7C_{43}H_{38}$ requires C 50.05, H 3.71%. Found C 49.77, H 3.73%.

$[Ru_3(\mu\text{-}C_2Bu^t)_2(\mu\text{-}PPh_2)_2(PPh_3)(CO)_6]$ (6). A solution of **4** (200 mg, 0.18 mmol) in thf (15 ml) was treated with PPh_3 (47 mg, 0.18 mmol) to give a bright yellow solution. Purification of the reaction mixture on a silica gel column gave a bright yellow band, which was crystallised (CH_2Cl_2–MeOH, slow evaporation) to yield yellow crystals of $[Ru_3(\mu\text{-}C_2Bu^t)_2(\mu\text{-}PPh_2)_2(PPh_3)(CO)_6]$ (**6**) (170 mg, 74 %). IR (cyclohexane): 2034s, 2009vs, 2002s, 1984w, 1971w, 1952s, 1941w. ^1H NMR: δ 7.58–6.91 (m, 35H, Ph); 1.22, 0.33 (2 × s, 2 × 9H, 2 × CMe_3). ^{13}C NMR: δ 201.66, 201.42, 200.11, 199.65, 199.30, 199.22 (6 × s, 6 × CO); 143.67–126.47 (m, Ph); 108.82 (t, J_{CP} = 14.9 Hz, C≡C); 105.55 (d, J_{CP} = 9.2 Hz, C≡C); 32.02, 29.52 (2 × s, 2 × CMe_3); 31.67, 30.01 (2 × s, 2 × CMe_3). ^{31}P NMR: δ 158.23 (d, J_{PP} = 142 Hz); 105.46 (d, J_{PP} = 142 Hz); 41.52 (s, PPh_3). FAB–MS: 1267, $[M]^+$; 1239, $[M - CO]^+$; 1183, $[M - 3CO]^+$; 1005, $[M - PPh_3]^+$. $Ru_3O_6P_3C_{60}H_{53}$ requires C 56.83, H 4.18%. Found C 56.53, H 4.08%.

Pyrolysis of $[Ru_3(CO)_{10}(Ph_2PC{\equiv}CPh)_2]$ (1b). A sample of $[Ru_3(CO)_{10}(Ph_2PC{\equiv}CPh)_2]$ (100 mg, 0.09 mmol) in thf (15 ml) was heated at reflux point for 90 min, then cooled. The solvent was removed and the residue purified by preparative TLC (10% CH_2Cl_2–hexane) to afford three bands. The top golden–yellow band (R_f 0.6) afforded $[Ru_3(CO)_7(\mu\text{-}\eta^1,\eta^2\text{-}C_2Ph)_2(\mu\text{-}PPh_2)_2]$ (**5b**) (20 mg, 20 %) following crystallisation (CH_2Cl_2–MeOH), the second bright red band contained the known diyne cluster $[Ru_3(CO)_7(\mu_3\text{-}\eta^2\text{-}PhC_2C{\equiv}CPh)(\mu\text{-}PPh_2)_2]$ (**7b**) (5 mg, 5%).[20] The third band (yellow) yielded $\{Ru_2[\eta^1,\eta^1\text{:}\ \eta^2,\eta^2\text{-}PhCC(PPh_2)CCPh](CO)_5\}(\mu\text{-}PPh_2)[Ru(CO)_3]$ (**8**) (38 mg, 39 %) following crystallisation from $CHCl_3$–MeOH. **5b** IR (cyclohexane): ν(CO) 2078m, 2028s, 2011w, 1968m cm^{-1}. ^1H NMR: δ 6.58–8.12 (m, Ph). ^{31}P NMR: δ 146.18 (d, J_{PP} = 155 Hz); 150.61 (d, J_{PP} = 155 Hz). FAB–MS 1044–876 $[M - nCO]^+$ (n = 1–7). $Ru_3O_7P_2C_{47}H_{30}$ requires C 52.61, H 2.80. Found C 52.43, H 2.92%. **8** IR (cyclohexane): ν(CO) 2091m, 2053s, 2038m, 2013m, 1999s, 1989s, 1969m, 1959m, 1930w cm^{-1}. ^1H NMR: δ 6.59–7.58 (m, Ph). ^{13}C NMR: δ 83.15 (d, J_{CP} = 4 Hz), 83.38 (d, J_{CP} = 4 Hz), 109.73 (s), 110.02 (s) (Ph*CCCC*Ph); 125.79–133.70 (m, Ph); 201.28, 202.87, 202.96, 203.08, 204.78, 204.86, 206.60, 206.64 (8 × s, 8 × CO). ^{31}P NMR: δ 16.48 (d, J_{PP} = 11 Hz); −77.89 (d, J_{PP} = 11 Hz). FAB–MS m/z 1100–876, $[M - nCO]^+$ (n = 0–8). $Ru_3O_8P_2C_{48}H_{30}$ requires C 52.36, H 2.73. Found C 52.41, H 2.74%.

Pyrolysis of $[Ru_3(CO)_{10}(Ph_2PC{\equiv}CBu^t)(Ph_2PC{\equiv}CPh)]$ (1c). A sample of $[Ru_3(CO)_{10}(Ph_2PC{\equiv}CBu^t)(Ph_2PC{\equiv}CPh)]$ (200 mg, 0.176 mmol) in toluene (15 ml) was heated at reflux point for 3 h. After this time the solvent was removed and the residue purified by preparative TLC (CH_2Cl_2–hexane: 1/5) to afford two main bands. The upper yellow band (R_f 0.8) afforded $[Ru_3(\mu\text{-}C_2Ph)(\mu\text{-}C_2Bu^t)(\mu\text{-}PPh_2)_2(CO)_7]$ (**5c**) (35 mg, 20%) following crystallisation (CH_2Cl_2–MeOH). The lower bright red band was crystallised ($CHCl_3$–MeOH) to give dark red blocks of $[Ru_3(\mu_3\text{-}\eta^2\text{-}PhC_2C{\equiv}CBu^t)(\mu\text{-}PPh_2)_2(CO)_7]$ (**7c**) (35mg, 20%). **5c** IR (cyclohexane): ν(CO) 2076s, 2025vs, 2021 (sh), 2008m, 2004m, 1967m, 1958m cm^{-1}. ^1H NMR: δ 1.07 (s, 6H, Bu^t, isomer 1), 0.02 (s, 3H, Bu^t, isomer 2); 6.77–8.11 (m, Ph). ^{13}C NMR: δ 32.67, 33.01 (2 × s, Bu^t, isomer 1), 30.16, 30.60 (2 × s, Bu^t, isomer 2); 94.72 (d, J_{CP} = 15 Hz), 94.97 (d, J_{CP} = 15 Hz), 95.46 (d, J_{CP} = 9.9 Hz), 104.03 (d, J_{CP} = 8.3 Hz), 109.06 (d, J_{CP} = 10 Hz), 110.72 (d, J_{CP} = 5.0 Hz), 116.90 (d, J_{CP} = 8.7 Hz) (*C*≡*C*, isomer 1 and 2); 128.06–142.57 (m, Ph); 193.65 (d, J_{CP} = 5.3 Hz), 194.00 (d, J_{CP} = 4.9 Hz), 194.67 (d, J_{CP} = 9.7 Hz), 195.11 (s), 195.45 (s), 195.72 (s), 198.44 (s), 199.26 (m), 200.28 (m), 200.72 (m) (all CO, isomer 1 and 2). FAB–MS m/z 1025–855 (M − nCO, n = 1–6). $Ru_3O_8P_2C_{45}H_{34}$ requires C 51.37, H 3.24. Found C 50.99, H 3.27%. **7c** IR (cyclohexane): ν(C≡C) 2058m ν(CO) 2021m, 2012s, 2002m, 1972m, 1953w cm^{-1}. ^1H NMR: δ 0.97 (s, 9H, CMe_3), 8.1–6.7 (m, 25H, Ph). ^{13}C NMR: δ 202.32, 198.47, 197.26, 187.26 (CO), 153.66–126.76 (Ph), 107.00, 90.22 (2 × s, 2 × C≡C), 30.94 (s, CMe_3), 28.58 (s, CMe_3). FAB–MS m/z 1100–876, $[M - nCO]^+$ (n = 0–8). $Ru_3O_8P_2C_{45}H_{34}$ requires C 51.37, H 3.24. Found C 51.72, H 3.28%.

Crystallography

Diffraction data were collected on Bruker SMART-CCD detector diffractometers using graphite monochromated Mo-Kα radiation (λ = 0.7107(3) Å). Data collections were carried out at 100 K(**1a**, **8**) and 173 K (**4**, **5a**–**c**, **6**, **7c**). Cell parameters were determined and refined using the SMART software[31] and raw frame data were integrated using the SAINT program.[32] Data were corrected for absorption by numerical integration based on measurements and indexing of the crystal faces using SHELXTL software (**1a**, **8**) and by the multi-scan method based on multiple scans of identical and Laue equivalent reflections using the SADABS program[33] (**4**, **5a**–**c**, **6**, **7c**). All structures were solved using direct methods and refined by full-matrix least squares on F^2 using SHELXTL.[34]

Hydrogen atoms were placed geometrically and allowed to ride on their parent C atom with U_{iso} (H) = 1.2 U and eq(C). Idealised C–H distances were fixed at 0.95Å (1.00Å for the C–H in the chloroform molecule). All non-hydrogen atoms were refined with anisotropic displacement parameters (adps). For the poorly resolved structure **1a** 15732 reflections measured, 7964 unique (R_{int} = 0.097) which were used in all calculations. The final $wR(F2)$ was 0.3122 (all data) and the final $R(F2)$ was 0.1379 (6756 observed data, $I > 2\sigma(I)$).

CCDC reference numbers 153694–153698, 172817 and 172818.

See http://www.rsc.org/suppdata/dt/b1/b108626j/ for crystallographic data in CIF or other electronic format.

Acknowledgements

This work was supported by grants from the National Research Council of Canada and NSERC (A.J.C), EPSRC and the University of Durham (P.J.L). P.J.L held an NSERC/NRC Canadian Government Laboratories Visiting Fellowship. J.A.K.H. thanks EPSRC for a Senior Research Fellowship. We thank Dr. Weibin Wang for preliminary crystallographic work.

Note added at proof: One of us (A.J.C) has recently described the synthesis of a diyne cluster *via* the coupling of the alkynyl moieties from RC≡CSC≡CR. (M. I. Alcalde, A. J. Carty, Y. Chi, E. Delgado, B. Donnadieu, E. Hernádez, K. Dallmann, and J. Sánchez-Nieves, *J. Chem. Soc., Dalton Trans.*, 2001, 2502.)

References

1 (*a*) S. Jeannin, Y. Jeannin, F. Robert and C. Rosenberger, *Inorg. Chem.*, 1994, **33**, 243; (*b*) M. I. Bruce, G. A. Koutsantonis and E. R. T. Tiekink, *J. Organomet. Chem.*, 1991, **407**, 391; (*c*) K. Yasufuku and H. Yamazaki, *Bull. Chem. Soc. Jpn.*, 1972, **45**, 2664; (*d*) S. J. Etches, I. J. Hart and F. G. A. Stone, *J. Chem. Soc., Dalton Trans.*, 1989, 2281.

2 (*a*) A. J. Carty, G. Hogarth, G. Enright and G. Frapper, *Chem. Commun.*, 1997, 1883; (*b*) J. E. Davies, M. J. Mays, P. R. Raithby and K. Sarveswaran, *Angew. Chem., Int. Ed. Engl.*, 1997, **36**, 2668.

3 Y. Chi, A. J. Carty, P. Blenkiron, E. Delgado, G. D. Enright, W. Wang, S.-M. Peng and G.-H. Lee, *Organometallics*, 1996, **15**, 5269.

4 B. J. Bobbie, N. J. Taylor and A. J. Carty, *J. Chem. Soc., Chem. Commun.*, 1991, 1511.

5 P. J. Low and M. I. Bruce, *Adv. Organomet. Chem.*, 2001, **48**, 71–288.

6 (*a*) P. Blenkiron, J. F. Corrigan, D. Pilette, N. J. Taylor and A. J. Carty, *Can. J. Chem.*, 1996, **74**, 2349; (*b*) J. F. Corrigan, S. Doherty, N. J. Taylor and A. J. Carty, *Organometallics*, 1992, **11**, 3160; (*c*) J. F. Corrigan, S. Doherty, N. J. Taylor and A. J. Carty, *Organometallics*, 1993, **12**, 1365; (*d*) P. Blenkiron, G. D. Enright, P. J. Low, J. F. Corrigan, N. J. Taylor, Y. Chi, J.-Y. Saillard and A. J. Carty, *Organometallics*, 1998, **17**, 2447; (*e*) P. Blenkiron, G. D. Enright, N. J. Taylor and A. J. Carty, *Organometallics*, 1996, **15**, 2855; (*f*) P. Blenkiron, G. D. Enright and A. J. Carty, *Chem. Commun.*, 1997, 483; (*g*) P. J. Low, G. D. Enright and A. J. Carty, *J. Organomet. Chem.*, 1998, **565**, 279; (*h*) P. J. Low, K. A. Udachin, G. D. Enright and A. J. Carty, *J. Organomet. Chem.*, 1999, **578**, 103; (*i*) P. J. Low, R. Rousseau, P. Lam, K. A. Udachin, G. D. Enright, J. S. Tse, D. D. M. Wayner and A. J. Carty, *Organometallics*, 1999, **18**, 3885.

7 (*a*) P. E. Garrou, *Chem. Rev.*, 1985, **85**, 171; (*b*) E. Sappa, A. Tiripicchio and P. Braunstein, *Chem. Rev.*, 1983, **83**, 203; (*c*) A. J. Carty, *Pure Appl. Chem.*, 1982, **54**, 113.

8 See, for example: (*a*) S. MacLaughlin, N. J. Taylor and A. J. Carty, *Organometallics*, 1983, **2**, 1194; (*b*) D. Nucciarone, S. A. MacLaughlin, N. J. Taylor and A. J. Carty, *Organometallics*, 1988, **7**, 106; (*c*) P. Blenkiron, G. D. Enright, P. J. Low, J. F. Corrigan, N. J. Taylor, Y. Chi, J.-Y. Saillard and A. J. Carty, *Organometallics*, 1998, **17**, 2447; (*d*) M. I. Bruce, M. L. Williams, J. M. Patrick and A. H. White, *J. Chem. Soc., Dalton Trans.*, 1985, 1229; (*e*) C. J. Adams, M. I. Bruce, E. Horn, B. W. Skelton, E. R. T. Tiekink and A. H. White, *J. Chem. Soc., Dalton Trans.*, 1993, 3299; (*f*) C. J. Adams, M. I. Bruce, E. Horn, B. W. Skelton, E. R. T. Tiekink and A. H. White, *J. Chem. Soc., Dalton Trans.*, 1993, 3313; (*g*) J. C. Daran, Y. Jeannin and O. Kristiansson, *Organometallics*, 1985, **4**, 1882 and references cited therein.

9 A. A. Cherkas, L. H. Randall, S. A. MacLaughlin, G. N. Mott, N. J. Taylor and A. J. Carty, *Organometallics*, 1988, **7**, 969.

10 A. J. Carty, N. J. Taylor and W. F. Smith, *J. Chem. Soc., Chem. Commun.*, 1979, 750.

11 A. A. Cherkas, N. J. Taylor and A. J. Carty, *J. Chem. Soc., Chem. Commun.*, 1990, 385.

12 E. Delgado, Y. Chi, W. Wang, G. Hogarth, P. J. Low, G. D. Enright, S.-M. Peng, G.-H. Lee and A. J. Carty, *Organometallics*, 1998, **17**, 2936.

13 D. K. Johnson, T. Rukachaisirikul, Y. Sun, N. J. Taylor, A. J. Canty and A. J. Carty, *Inorg. Chem.*, 1993, **32**, 5544.

14 S. Rivomanana, G. Lavigne, N. Lugan and J.-J. Bonnet, *Organometallics*, 1991, **10**, 2285 and references therein.

15 A. J. Carty, S. A. MacLaughlin and N. J. Taylor, *J. Organomet. Chem.*, 1981, **204**, C27.

16 M. I. Bruce, B. K. Nicholson and M. L. Williams, *Inorg. Synth.*, 1989, **26**, 221.

17 (*a*) M. I. Bruce, M. J. Liddell, C. A. Hughes, J. M. Patrick, B. W. Skelton and A. H. White, *J. Organomet. Chem.*, 1988, **347**, 181; (*b*) T. Chin-Choy, N. L. Keder, G. D. Stucky and P. C. Ford, *J. Organomet. Chem.*, 1988, **346**, 225.

18 K. W. Lee, W. T. Pennington, A. W. Cordes and T. L. Brown, *J. Am. Chem. Soc.*, 1985, **107**, 631.

19 J. F. Corrigan, Y. Sun and A. J. Carty, *New J. Chem.*, 1994, **18**, 77.

20 J. F. Corrigan, M. Dinardo, S. Doherty and A. J. Carty, *J. Cluster Sci.*, 1992, **3**, 313.

21 F. Van Gastel, S. A. MacLaughlin, M. Lynch, A. J. Carty, E. Sappa, A. Tiripicchio and M. Tiripicchio-Camellini, *J. Organomet. Chem.*, 1987, **326**, C65.

22 For examples see: (*a*) A. J. Deeming, M. S. B. Felix and D. Nuel, *Inorg. Chim. Acta*, 1993, **213**, 3; (*b*) M. I. Bruce, P. J. Low, A. Werth, B. W. Skelton and A. H. White, *J. Chem. Soc., Dalton Trans.*, 1996, 1551; (*c*) J. Lewis, B. Lin, M. S. Khan, R. A. Al-Mandhury and P. R. Raithby, *J. Organomet. Chem.*, 1994, **484**, 161.

23 M. Kersting, K. Dehnicke and D. Fenske, *J. Organomet. Chem.*, 1986, **309**, 125.

24 J. A. Cabeza, I. del Rio, S. Garcia-Granda, M. Moreno, V. Riera, M. de J. Rosales-Hoz and M. Suarez, *J. Inorg. Chem.*, 2001 in press.

25 (*a*) H. Werner, O. Gervert, P. Steinert and J. Wolf, *Organometalics*, 1995, **14**, 1786; (*b*) J. Lewis, B. Lin and P. R. Raithby, *Trans. Met. Chem.*, 1995, **20**, 569; (*c*) M. I. Bruce, B. W. Skelton, A. H. White and N. N. Zaitseva, *J. Chem. Soc., Dalton Trans.*, 1996, 3151; (*d*) S. M. Waterman, M. G. Humphrey, V.-A. Tolhurst, M. I. Bruce, P. J. Low and D. C. R. Hockless, *Organometallics*, 1998, **17**, 5789; (*e*) M.-C. Chung, A. Sakurai, M. Akita and Y. Moro-oka, *Organometallics*, 1999, **18**, 4684; (*f*) M. I. Bruce, J.-F. Halet, S. Kahal, P. J. Low, B. W. Skelton and A. H. White, *J. Organomet. Chem.*, 1999, **578**, 155; (*g*) M. I. Bruce, B. C. Hall, B. D. Kelly, P. J. Low, B. W. Skelton and A. H. White, *J. Chem. Soc., Dalton Trans.*, 1999, 3719.

26 M. I. Bruce, N. N. Zaitseva, B. W. Skelton and A. H. White, *J. Organomet. Chem.*, 1997, **536–537**, 93.

27 A. J. Carty, S. A. MacLaughlin and D. Nucciarone, in *Phosphorus-31 NMR Spectroscopy in Stereochemical Analysis, Organic Compounds and Metal Complexes*, eds. J. G. Verkade, L. D. Quinn, (Methods in Stereochemical Analysis 8) VCH, Deerfield Beach, FL, 1987, pp. 559–619.

28 (*a*) M. I. Bruce, J. G. Matisons, B. W. Skelton and A. H. White, *J. Organomet. Chem.*, 1983, **251**, 249; (*b*) A. Astier, J.-C. Daran, Y. Jeannin and C. Rigault, *J. Organomet. Chem.*, 1983, **241**, 53; (*c*) A. A. Kordize, A. I. Yanovsky and Yu. T. Struchkov, *J. Organomet. Chem.*, 1992, **441**, 277.

29 For related chemistry see (*a*) J. E. Davies, M. J. Mays, P. R. Raithby, K. Sarveswaran and G. A. Solan, *J. Chem. Soc., Dalton Trans.*, 2000, 3331; (*b*) J. E. Davies, M. J. Mays, P. R. Raithby, K. Sarveswaran and G. A. Solan, *J. Chem. Soc., Dalton Trans.*, 2001, 1269 and references therein.

30 A. J. Carty, N. K. Hota, T. W. Ng, H. A. Patel and T. J. O'Connor, *Can. J. Chem.*, 1971, **49**, 2706.

31 SMART-NT, Data Collection Software, Version 5.0, Bruker Analytical X-ray Instruments Inc., Madison, WI, 1998.

32 SAINT-NT, Data Reduction Software, Version 5.0, Bruker Analytical X-ray Instruments Inc., Madison, WI, 1998.

33 G. M. Sheldrick, SADABS, Empirical Absorption Correction Program, University of Göttingen, 1998.

34 SHELXTL, Version 5.1, Bruker Analytical X-ray Instruments Inc., Madison, WI, 1998.